HOT NEUTRONS AND THEIR APPLICATIONS AT FRM II REACTOR

V. HUTANU, A. RÖHRMOSER, C. MÜLLER, M. FUSS, A. PICHLMAIER
Forschungs-Neutronenquelle Heinz Maier-Leibnitz (FRM II), TU München, Lichtenbergstr. 1, D85747 Garching b. München - Germany

M. MEVEN
Institute of Crystallography, RWTH Aachen University and Jülich Centre for Neutron Science (JCNS) at Heinz Maier-Leibnitz Zentrum (MLZ), Lichtenbergstr. 1, D85747 Garching - Germany

L. PETERS, G. ROTH
Institute of Crystallography, RWTH Aachen University Jägerstr. 17-19, D52066 Aachen - Germany

ABSTRACT

Neutrons with energies between 0.1 and 1 eV slightly above the typical thermal spectrum of a research reactor, often-called hot neutrons, are valuable probes for different scientific applications. Their use in the neutron diffraction, spectroscopy, absorption or irradiation experiments often provides results of superior quality in comparison to thermal neutrons or even results unreachable by the use of the latter. At FRM II, hot neutrons are generated by a dedicated secondary source in the moderator tank, which shifts the spectrum of the moderated neutrons towards higher energies. A beamline with two channels pointing to the centre of the hot source extracts the re-moderated neutrons towards the two dedicated experimental installations POLI and HEiDi. Here, we present the design of the hot neutron source and related instrumentation. In addition, a few representative examples of their use from the fields of crystallography, magnetism and nuclear physics are shown to demonstrate their usefulness.

1. Introduction

Neutrons with wavelengths between 0.5 and 0.9 Å and mean energies of about 200 meV, often called hot neutrons, are important and very useful probes for scientific studies in different fields of research like condensed matter physics but also many others. By the scattering processes the hot neutrons provide larger energy and impulse transfer then the thermal or cold ones. Thus, they open the possibility to increase the accessible region in the reciprocal space (space of the impulse transfer). As the internal structure of the studied object can be obtained by the inverse Fourier transformation of the scattering cross-section, it is logical to conclude, that the real structure of the studied object can be determined with better resolution if the experimental data will be obtained up to the larger region of the reciprocal space. Hot neutrons bear also other advantages compared to the thermal ones: they have a lower incoherent background by the scattering on hydrogen, a lower negative effect of the primary extinction and a lower absorption of strongly absorbing materials like Gd or other rare-earth containing compounds. Some elements (isotopes) possess resonances just in the same energy region. This makes it possible to apply hot neutrons for so-called anomalous dispersion (wavelength dependent scattering) in order to solve the phase problem in the structural research. Also, resonance nuclear absorption is of significant scientific interest as it may provide different quantum-mechanical states then in the overaged thermal spectrum.

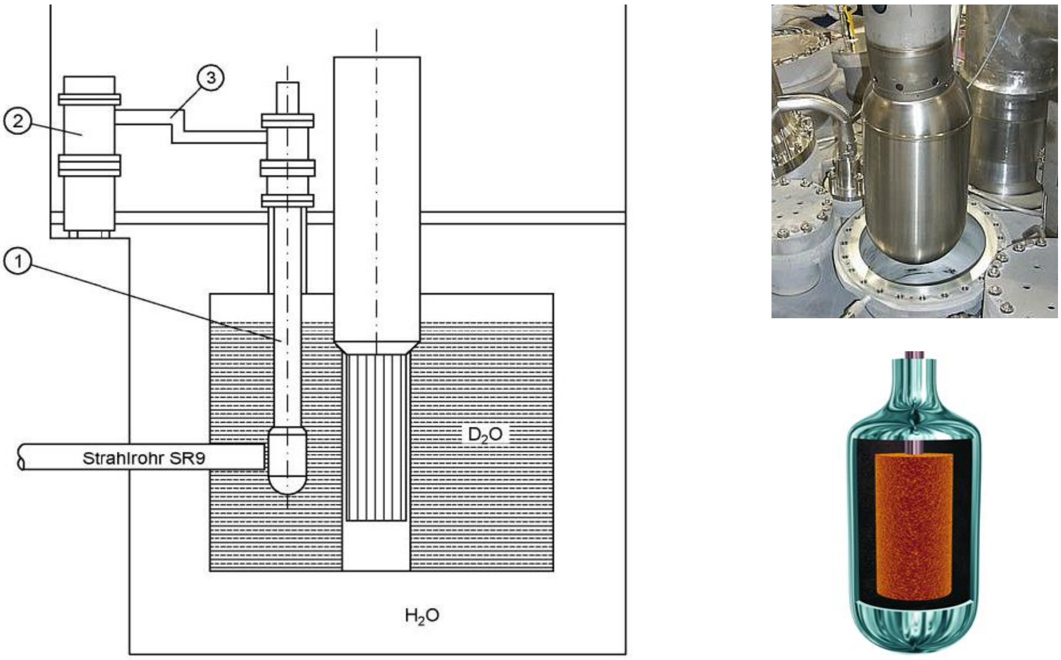

Fig. 1, left: Schematic drawing of the HNS installation. Numbering in the figure denotes: 1 – in-pile part in the moderator tank, 2 – external instruments box in the reactor pool, 3 – double wall connecting tubing. Top right: photograph of the hot source Zircaloy container, bottom right: sketch of the graphite moderator block inside container.

Generally, in a typical reactor thermal neutrons with wavelengths of 1 to 4 Å are generated. The part of the hot neutrons is very low. It can be increased if the temperature of the moderator reaches 2000-2500°C. Such an additional solid graphite moderator is called a hot neutron source (HNS). To our knowledge, the first HNS was installed at the high-flux reactor at the Institute Laue Langevin (ILL) in Grenoble, France in the early 70th [1]. Between 1980 and 2019 another HNS was successfully operated at the reactor Orphée in Saclay, France. In 2004 a HNS was implemented also at the at that time new reactor FRM II in Garching, Germany [2, 3]. To the best of our knowledge, nowadays the HNSs at ILL and FRM II are the only two available sources for the scientific communities interested in hot neutrons worldwide. There exist plans for the implementation of a new HNS also on the other reactors in the next future like PIK in Russia [4], ANSTO (Australia) [5] or Dhruva (India) [6] and maybe others as well. In this perspective, the present report aims to share the experience gained at FRM II in the development and exploitation of the HNS and related instrumentation as well as to demonstrate the power and usefulness of hot neutrons for physics investigations hardly possible with other techniques.

2. Hot neutron source

2.1 The overall design

The core element of the hot source represents a graphite moderator of 200 mm in diameter and 300 mm in length weighting about 15 kg (Fig. 1, right bottom) situated at about 42 cm from the centre of the fuel element in radial distance and at the same height (Fig. 1, left). The moderator is heated by the prompt gamma radiation arising in the fuel element up to 2050°C. Thus, the hot source re-moderates the thermal neutrons in the moderator tank to speed them up. The moderator is thermally isolated by carbon fibres and placed into a double wall container made of Zircalloy to minimise neutron absorption (Fig. 1, right top). The space between the walls is filled with He, the inner volume is flooded with a He/Ne gas mixture to reduce thermal conduction. Several temperature sensors monitor the temperature of the moderator [7]. The container is fixed to the lower part of the holding tube integrated into the moderator tank top flange. Over this tube and connecting tubing 3 (Fig. 1, left) all the gas supply and control cabling is provided from the external box 2 (Fig. 1, left). The holding tube is flooded with D_2O in the moderator tank to reduce gamma radiation upwards from the hot source. The connecting tubing 3 is filled with He. A number of auxiliary equipment like pressurised air for pneumatic components control, the N_2, He, Ne gases supply as well as vacuum pumps and an exhaust gas handling system support the functioning of the hot source. More technical details about the FRM II HNS are published elsewhere, e.g. [8, 9].

2.2 Beam tube

The double channel beam tube SR9 performs the extraction of re-moderated hot neutrons from the moderator tank and their transport to the instruments in the experimental hall. Two windows of 80x120 mm^2 width x heights are provided for the two beam channels of 7.5° inclination to each other pointing to the centre of the source. Both channel cross sections diverge slightly from the source toward the application. Downstream on the beam flow, focused monochromators are installed at both channels to maximise the useful flux density at the sample positions and to select the requested neutron energy. The size of the source window, channel cross section and length of the flight path from the incoming window to the monochromator define the maximum intrinsic collimation of the incoming beam. For channel SR9A (POLI), e.g. a horizontal beam collimation between 0.35° and 0.75° can be achieved using variable slits in front of the monochromator. On the other side of the beam tube, close to the outer reactor-pool wall, a massive rotating revolver beam shutter provides variable openings for the channels. Four positions of the shutter are available per motor control: only channel A or B open, both A and B open or both closed.

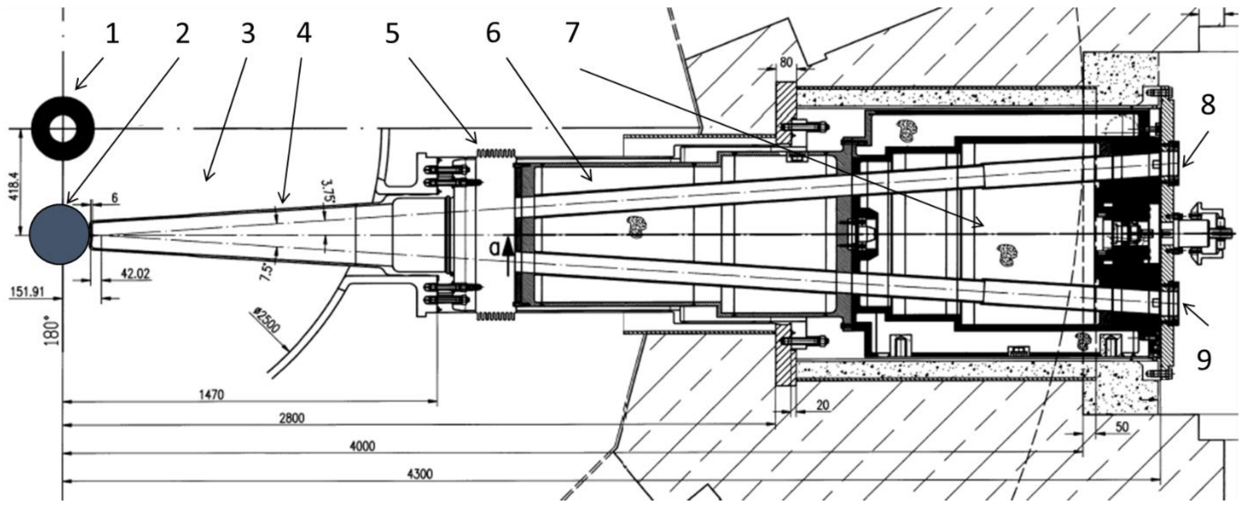

Fig. 2: Cross section top view of the beam tube SR9 to extract re-moderated neutrons from the hot source towards experimental stations. Numbering in the figure denotes: 1- fuel element in the reactor core, 2 - hot source, 3 – heavy water moderator tank, 4 – Al beam tube's nose in the moderator tank, 5 – light water reactor pool, 6 – fixed double channel beam tube, 7 – rotating revolver beam shutter, 8 – beam channel SR9A towards POLI, 9 – beam channel SR9B towards HEiDi station respectively.

2.3 Spectrum shift

The neutron flux, spectral and angular distribution at the entrance window of the beam tube SR9, pointing toward the hot source, were calculated using the MCNP code [10] for different temperatures of the hot source and compared with the real measurements on the beam line SR9B (HEiDi). Fig. 3 left shows wavelength (energy) dependent flux densities calculated for two temperatures of the HNS: 300 K (thermal spectrum without hot source), and 2000 K (temperature of the sensor inside the graphite moderator after full thermalisation at the nominal reactor power of 20 MW). The scale on the left hand side shows the absolute neutron flux density values (blue symbols). The scale on the right hand side displays the gain factor (brown line). It is easy to observe that for a wavelength shorter than 0.9 Å a significant increase in the flux density with hot source is realised. The maximum is reached at 0.5 Å where the flux increases by more than one order of magnitude. Fig. 3 right top denotes the time evolution of the reactor power (orange symbols) and of the measured temperature in the HNS (blue symbols) during the test experiment on HEiDi in 2006. At about 13:30 (after 4.5 hours of slow ramping up) the reactor reaches it nominal power of 20 MW. At that time, HNS temperature is of about 1200°C. It requires another 8-9 hours to fully thermalise the HNS at the nominal reactor power, due to the significant size and mass of the solid moderator. Fig. 3 right bottom shows measured normalised counting intensities for the 0.55 Å wavelength neutrons as function of reactor power. The effect of the HNS heating with time is clearly visible by the gradual increase of the counting rates for the hot neutrons at the certain discrete values of the reactor power (e.g. 4, 15, 19, 20 MW correspondingly) and correlates well with the above data. Approximating the obtained experimental dependence by a simple exponential behaviour one results in the rough intensity gain by a factor larger than 11 in good agreement with MCNP calculations (Fig. 3 left). The simulations show that in the same time the flux density in the thermal part of the spectrum (above 1 Å) decreases. This decrease was also experimentally observed by the measurements with 1.17 Å neutrons on HEiDi. However, the absolute value of the measured intensity with this wavelength in only slightly diminished (about 20%), because the positive effect of increased reflectivity of the monochromator at longer wavelength partially compensates the flux reduction. Thus, sufficiently high flux density is still available for experiments with thermal neutrons up to 1.2-1.4 Å at the same beam channel with HNS.

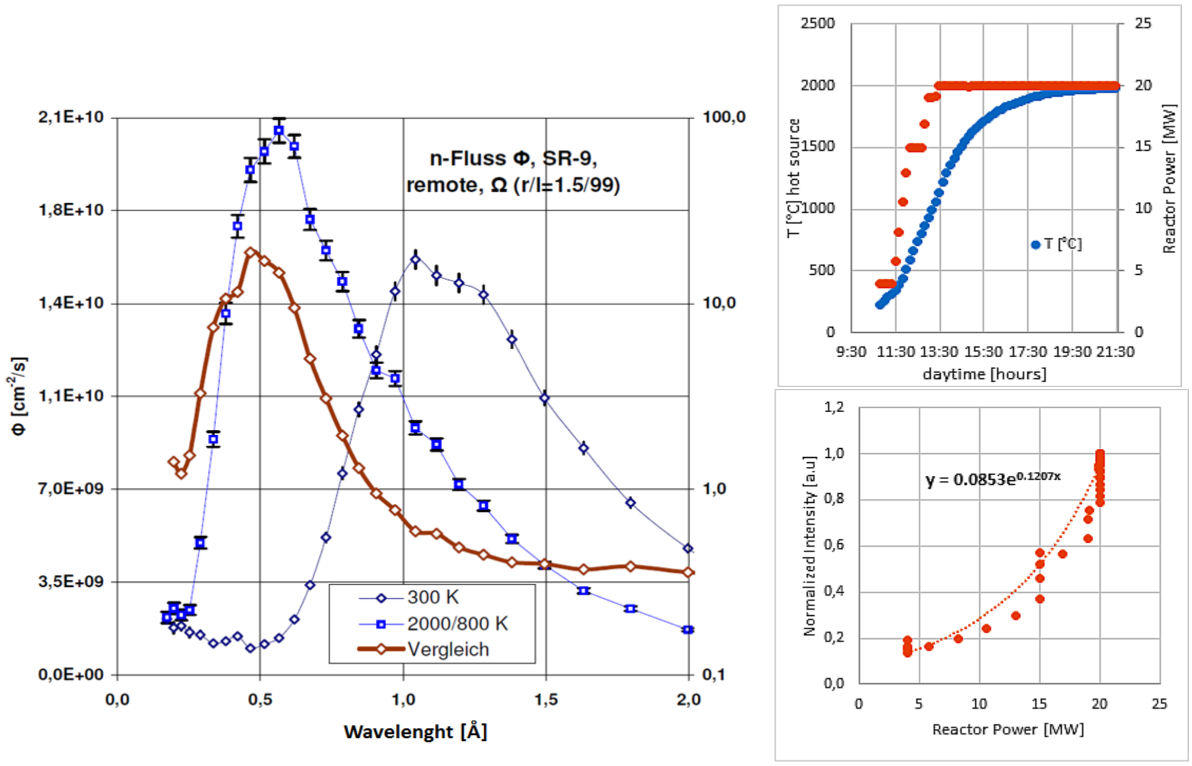

Fig. 3, left: Calculated neutron flux density at the window of SR9 with HNS at 300 K - water moderator temperature and 2000 K - hot graphite moderator temperature at 20 MW (blue symbols, left-side scale), brown symbols denote the wavelength dependent gain factor (right-side scale). Top right: Time evolution of the reactor power (orange symbols) and of the corresponding temperature in the HNS (blue symbols) during the test experiment on SR9B. Bottom right: measured normalised intensity at 0.55 Å neutrons as function of thermal reactor power during the same experiment.

3. Instrumentation for hot neutrons

At the ILL in Grenoble there are three beam channels pointing toward their HNS with totally four neutron scattering instruments installed: D3, a single crystal diffractometer with polarised neutrons, D9, a four-circle single crystal diffractometer, D4, a disordered materials diffractometer and IN1, a triple axis spectrometer for large energy excitations. At the MLZ in Garching two beam channels are provided with hot neutrons supplying two single crystal diffractometers: HEiDi, the non-polarised four-circle diffractometer, and POLI, the one with polarised neutrons and normal beam geometry.

3.1 HEiDi (**H**eißes **Ei**nkristall **Di**ffractometer)

The single-crystal diffractometer HEiDi is situated at the beam channel SR9B at a distance of about 6.63 m between the hot source and the monochromator of the instrument. It uses unpolarized neutrons with wavelengths between 1.4 Å and 0.5 Å by Bragg reflections from dedicated variably-vertically-focused monochromators [11, 12]. By using hot neutrons the diffractometer is designed for high-resolution crystal structure analyses in a large reciprocal space area $Q = \sin(\theta)/\lambda$ (where θ is the scattering angle and λ is the neutron wavelength). In addition, crystal structure investigations are possible in-situ in a wide temperature range between 2.5 K and 1300 K and, most recently, also at high pressures up to 5 GPa. Thus, temperature and/or pressure induced phase transitions can be studied over a wide range. Typical scientific questions cases include the precise determination of hydrogen positions and -bonds in molecules and framework structures or of other light elements, e.g. Li or O in corresponding ion conductors. These cases typically cannot be adressed by X-ray diffraction experiments. Often, corresponding structures are studied in connection with anharmonic thermal oscillations of their atoms, defects, or static/dynamic disorder phenomena. Another focal point of interest is the determination of magnetically ordered states, and incommensurately modulated structures. HEiDi has been in user operation since 2005. More than 100 scientific publications have been published using results measured on HEiDi. It participates regularly in educational activities concerning young researchers in the field of neutron diffraction (TUM, RWTH, JCNS and HEREON lab courses and schools as well as the European MaMaSELF Erasmus Mundus Program). Many theses of graduate and postgraduate students from all over the world have been successfully completed using results from HEiDi.

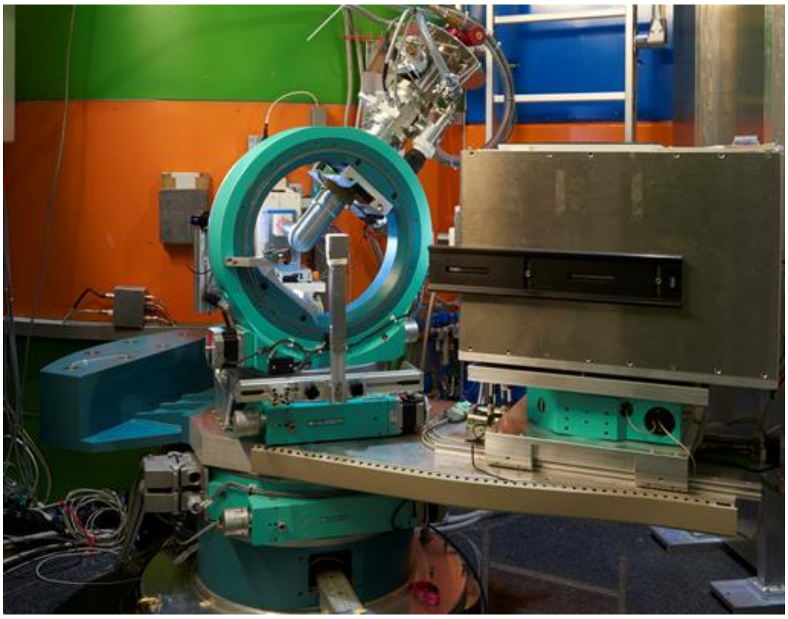

Fig. 4: Single crystal diffractometer HEiDi at beam channel SR9B.

3.2 POLI (**Pol**arisation **I**nvestigator)

The single-crystal diffractometer with polarised neutrons POLI is located at the beam channel SR9A at a distance of about 8.14 m between the hot source and its monochromator. The main difference between POLI and other polarised hot instruments like D3 (at ILL) is the following: they are using Cu_2MnAl single crystal polarisers merging both the energy selection and neutron polarisation function in one device. Cu_2MnAl polarisers work well with thermal neutrons but have some drawbacks like lower reflectivity and inferior resolution when used with hot neutrons. Moreover, using them it becomes difficult to create a focused geometry as the crystals are situated in a strong magnetic field to provide sufficiently high neutron polarisation. In contrast, POLI is using non-polarised variably-double-focused monochromators in combination with dedicated polarisers. This concept of decoupling neutron optics from the polarisation function permits to maximise the available neutron flux density at the sample position while maintaining the high resolution and polarisation degree for the different available wavelengths between 0.55 Å and 1.15 Å at the same time [13, 14]. POLI is designed to host bulky and heavy sample environments like cryomagnets, furnaces, polarimeters, etc. This allows the investigation of samples under extreme conditions like very low/high temperatures (between 0.04 K and 2100 K), large magnetic fields (up to 12 T), electric fields (up to 10 kV), pressures (2.5 GPa) and their combinations for multi-parameter studies on advanced functional materials. Two polarised neutron diffraction techniques namely Flipping Ratio (FR) in high magnetic fields (up to 8 T) [15] and spherical neutron polarimetry (SNP) in zero magnetic field (10^{-7} T) [16] are implemented for detailed investigations on the magnetism at the atomic level. Polarised hot neutrons are useful not only for studies on magnetism, but may also be applied to study the fundamental asymmetries in the nuclear reaction of heavy ions. So called parity violation effects like TRI and ROT in the fission of ^{235}U at different energies close to the first resonance at 270 meV were measured and are presented in more detail in the following chapter. The instrument POLI started user operation in 2015. Since then, more than 45 scientific papers have been published using results measured on POLI. These have actively contributed to the successful completion of numerous PhD and Master's theses.

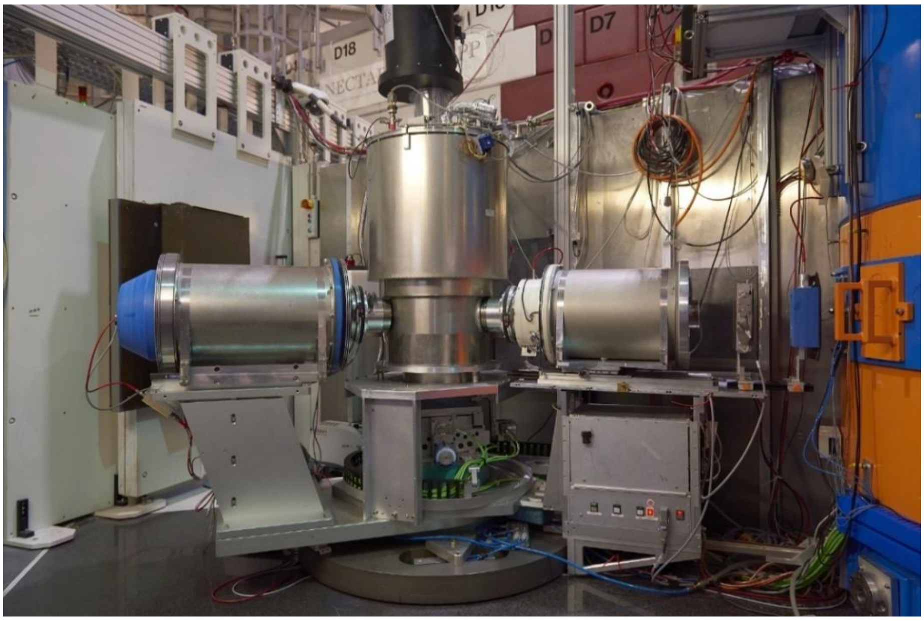

Fig. 5: Polarised single crystal diffractometer POLI with SNP setup [16] at the beam channel SR9A.

4. Selected application examples

4.1 Precise determination of crystal structure parameters with hot neutrons

As mentioned in the previous section 3.1 the available Q-range is inversely proportional to the used wavelength. Thus, with the limited maximal detector angle, the number of accessible Bragg reflections measurable for the precise determination of the crystallographic parameters increases significantly when using shorter wavelengths. The completeness of the measured datasets leads to a much higher precision in the determination of the essential parameters both of the crystal structure (symmetry) like the fractional coordinates and the physical properties of the material, namely the displacement parameters of the atoms. As an example, measurements on Cobalt-olivine, Co_2SiO_4 taken on HEiDi with hot neutrons (λ = 0.552 Å), demonstrate the determination of the *x* coordinate of one of the Co-atoms within the CoO_6-octahedra in the orthorhombic structure, interconnected by edge-sharing with SiO_4-tetrahedra (Fig. 6 right). A large data set with 1624 independent reflections up to $Q = \sin(\theta)/\lambda = 1.05$ Å^{-1} was measured. Then, the data were cut off successively in shells of $\sin(\theta)/\lambda$ and the resulting partial data sets were used to analyse the resolution-dependent variation of the structural parameters. The resulting atomic coordinate x_{Co2} with related error is plotted as a function of *Q* in Fig. 6 (left). The precision improves significantly with increasing ($\sin(\theta)/\lambda$), as is evident from the decreasing size of the error bars. Additionally, there are apparently oscillations of the value of the atomic coordinate, which only diminish at high data resolution. This high d_{hkl}-value resolution that can be obtained from hot neutron diffraction is also useful to derive precise temperature dependent displacement parameters [17, 18]. In addition, the quality of such data often allows for refining anharmonic displacement parameters, applicable when the harmonic approximation, which is the basis of the description of thermal displacements by the Debye-Waller factor, fails. A non-parabolic potential at the site of the vibrating atom was found e.g. in [19].

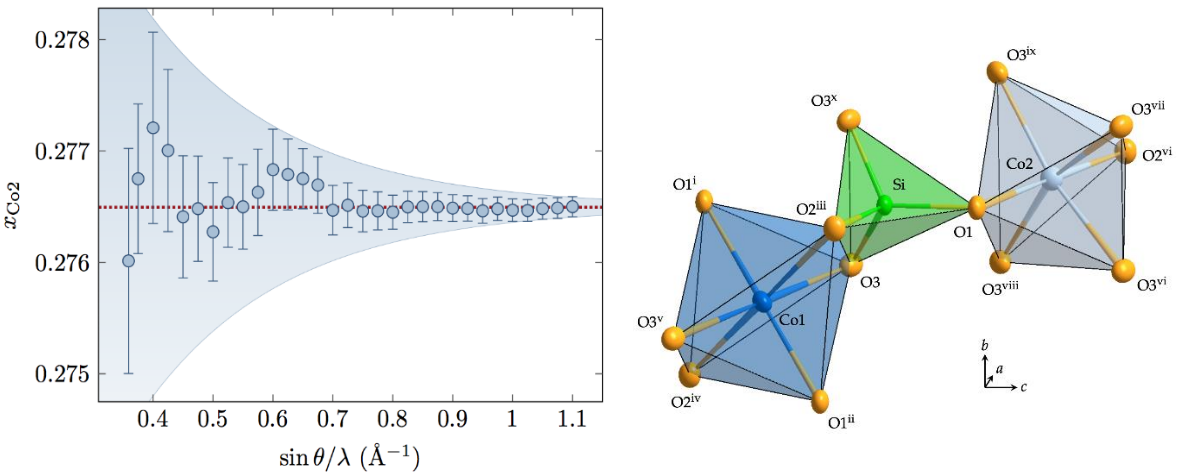

Fig. 6: left: Refined values and error bars of the *x* coordinate of Co2 in Co_2SiO_4 as a function of the $\sin(\theta)/\lambda$ data range from single-crystal neutron diffraction. Right: clinographic view of the CoO_6 and SiO_4 polyhedra in Co_2SiO_4 at room temperature [9].

4.2 Magnetic structure determination in $CeRhIn_5$ on absorption-optimised samples

Thermal neutrons have a penetration depth of several cm in most materials, making them suitable probes for typical neutron diffraction samples of a few mm in size. However, studying magnetic properties in rare earth elements (or other strongly absorbing elements like ^{10}B,

^{113}Cd, etc.) containing compounds may be particularly challenging. The strong scattering angle-dependent absorption may compromise the obtained results significantly, especially, if the expected magnetic signals are weak. Usually, the absorption cross section scales with the power law of neutron energy. Thus, using hot neutrons permits the reduction of parasitic absorption effects by optimisation of sample size and geometry. For example, in the heavy fermion superconducting material $CeRhIn_5$ a variety of values for the ordered magnetic moment at low temperatures were reported in the literature based on measurements using thermal neutrons. Values span between 0.25 and 0.95 μ_B per Rh atom depending on the used samples, wavelengths, etc. [20]. However, the knowledge of the precise value of the partially ordered moment is extremely important from the theoretical point of view in order to adopt a specific microscopic model for the collective electronic behaviour and superconductivity at low temperatures. Careful inspection of all reported data revealed the fact, that most of them were obtained from large single crystals significantly exceeding the absorption length for the in the sample contained indium and the used neutron wavelength. Thus, those data were in need of a thorough absorption correction, which would probably alter significantly the resulting value of the weak magnetic moment. In fact, a new experiment on POLI using polarised and non-polarised hot neutrons on an absorption-optimised sample in order to avoid this effect resulted in an ordered moment of 0.54(8) $\mu_{B/}$Rh [20]. This provided an improved basis for the theoretical description of that intriguing material and the discovery of emergent tunable heterostructures with potential applications in quantum materials [21]. The usefulness of hot neutrons for absorption reduction during the investigation of the magnetism in rare earth elements containing compounds has been successfully demonstrated for several other topic functional materials measured at the diffractometer HEiDi, including multiferroic $GdMnO_3$ [22] and antiferromagnetic and superconducting $EuFe_2As_2$ compounds, respectively [23, 24].

4.3 Measuring the parity non-conservation effects in the neutron induced fission of heavy nuclei

The search for the violation of time reversal invariance (TRI) is one of the main open questions in modern physics and our understanding of the visible universe. In Ref. [25] the idea was proposed to look for such symmetry violations in the fission of heavy nuclei. Later a pronounced anisotropy in the emission of an alpha-particle in the ternary fission of U in dependence on the direction of the neutron spin and the fragment momentum was experimentally found (TRI-effect) [26]. Moreover, it was noticed that by reversing the direction of polarization of the neutron beam, the angular distribution of the α- particles is shifted by a small angle relative to the axis of fragment emission. The authors called this effect the ROT effect [27]. Later both TRI and ROT effects for fission neutrons and gamma quanta have been successfully observed also in the binary fission of different U and Pu isotopes [28,29]. Active research in this field lead to the conclusion that both, TRI and ROT effects are only apparently related to the time reversal violation, but indeed have no direct connection with the violation of the time reversal invariance and can be explained solely by the quantum mechanical mechanism of the fission process. According to Ref. [30], both effects depend on the quantum numbers J and K, which characterize the fission channel. It was proposed to use such asymmetry measurements as a new spectroscopic method to learn about the quantum states in the exited nucleus just immediately before the fission process. However for the thermal (or cold) neutron induced fission (where all previous data were obtained), there is a mixture of several spin states, and the weights of these states are unknown. The only way to get "clean" data is to perform measurements on isolated resonances. Fortunately, the lowest resonances of both ^{233}U and ^{235}U are well within the energy spectrum of the HNS at FRM II. Furthermore, using, e. g. the Cu (220) monochromator on POLI, a polarised neutron beam with an energy of 0.27 eV (lowest resonance ^{235}U) may be easily reached [31]. Energy dependent asymmetry measurements for the ROT effect in neutron and gamma emission for ^{235}U were successfully performed [32-35]. Experiments with other isotopes like ^{233}U or ^{139}La need a slight adjustment of the available beam pathway and are planned for the future. At present, there are several theoretical models trying to describe both effects. The results of our experiments on ^{235}U are in good agreement with the exhaustive theoretical model from [21]. Fig. 7 shows the experimental setup used for the resonant absorption experiment on POLI [30].

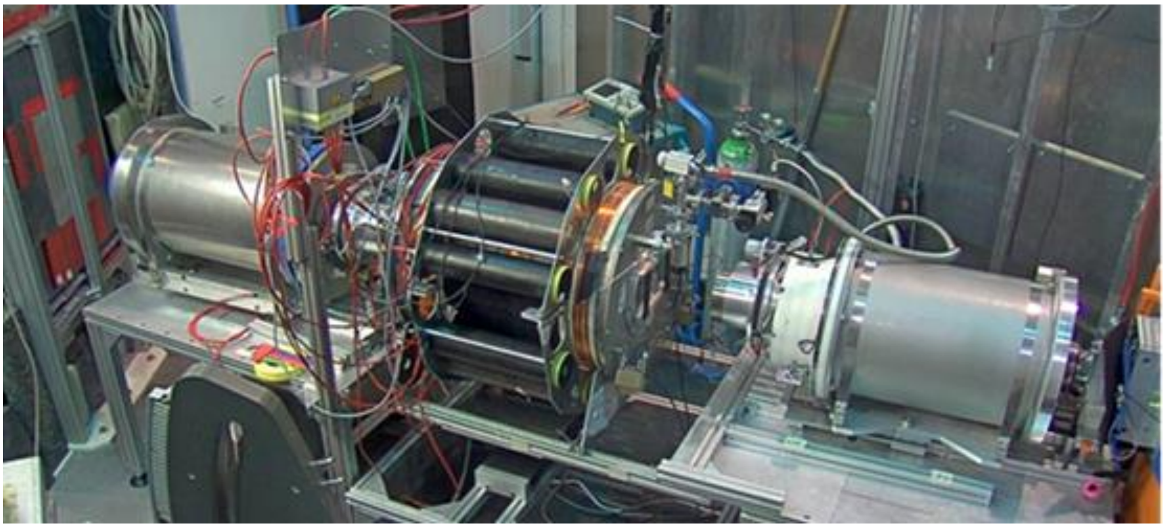

Fig. 7: Setup for measuring parity non-conservation effects in the neutron induced fission of ^{235}U using thermal and hot polarized neutrons on the beamline POLI at MLZ.

5. Conclusion

Hot neutrons available from reactor-based sources are rather rare but extremely useful and valuable probes for the research in different fields of science. Used in spectroscopy, diffraction, absorption or irradiation they can provide information inaccessible with “standard” thermal neutrons or other types of radiation. At FRM II a dedicated powerful source for the production of hot neutrons was successfully implemented and operates reliably since then. It allows the increase of the useful neutron flux density in the short-wavelength region by about one order of magnitude. The source itself is assisted by a dedicated set of instrumentation which allows the use of the intense neutron beams required and optimised for certain energies for different scientific applications. The design and main technical parameters of the secondary source, dedicated beam tubes and the well adopted instrumentation at the beam channels SR9A and SR9B was presented. The listed examples bear witness for the overall high performance of the entire installation and its worldwide unique features (e.g. polarised hot neutrons).

Acknowledgements

We are thankful to W. Luberstetter for technical support. The instrument POLI has been supported by German Ministry for Education and Research BMBF through the projects: 03HE6AA3, 03HE7AAC, 05KN7PAA, and 05K10PA2. Both instruments HEiDi and POLI are operated at MLZ by RWTH Aachen University in cooperation with FZ Jülich (Jülich-Aachen Research Alliance JARA).

6. References

[1] P. Ageron “Optimisation de le position et des demensions d'une source” ILL Annual Report 1974, Grenoble, p. 38.
[2] C. Müller, E. Gutsmiedl, A. Röhrmoser, A. Scheuer, Proc. IGORR 10, Washington (USA), September 2005, https://www.igorr.com/Pages/Proceedings/Washington-2005.aspx
[3] E. Gutsmiedl, C. Müller, A. Scheuer, TUM, ZWE FRM-II Annual Report 2004, p. 21, https://www.frm2.tum.de/frm2/aktuelles-medien/broschueren/jahresberichte/
[4] I. V. Golosovsky, Yu. A. Kibalin, A. K. Ovsyanikov, PNPI Preprint № 2977, 06.07.2015 (in Russian)
[5] Capabilities of OPAL, http://www.ansto.gov.au/AboutANSTO/OPAL/Capabilities/#sthash.6GVFvCqw.dpuf
[6] Barc Technical Brochures. http://www.barc.gov.in/publications/tb/nfnbr- book-R.pdf
[7] C. Müller, H. Gerstenberg, E. Gutsmiedl, RRFM 2011 Transactions https://inis.iaea.org/search/search.aspx?orig_q=RN:42043841
[8] C. Müller, E. Gutsmiedl, A. Scheuer, Proc. IGORR 8 Meeting, Munich (Germany), April 2001, https://www.igorr.com/Pages/Proceedings/Munich-2001.aspx
[9] C. Müller, E. Gutsmiedl, TUM, ZWE FRM-II Annual report 2002, p. 63-66, https://www.frm2.tum.de/frm2/aktuelles-medien/broschueren/jahresberichte/
[10] T. Goorley, et al. Nuclear Technology, 180, pp 298-315 (2012).
[11] M. Meven, V. Hutanu, G. Heger, Neutron News 18(2), 19-21 (2007).
[12] M. Meven, A. Sazonov, J. Large-scale Res. Facilities 1, A7.(2015).
[13] V. Hutanu, M. Meven, G. Heger, Physica B 397, 135-137 (2007).
[14] V. Hutanu, J. Large-scale Res. Facilities, 1, A16. (2015).
[15] V. Hutanu, H. Thoma, et al. IEEE Trans. Magn. (in press) (2021).
[16] V. Hutanu, W. Luberstetter, E. Bourgeat-Lami, et al. Rev. Sci. Instr. 87, 105108 (2016).
[17] M. Meven, G. Roth, “Neutron diffraction” Handbook of solid state chemistry / edited by R. Dronskowski, Sh. Kikkawa and A. Stein. - Volume 3: Characterization, Weinheim : Wiley-VCH Verlag GmbH & Co. KGaA, 3 3, 77-108 (2017) [10.1002/9783527691036.hsscvol3004]
[18] A. Sazonov PhD Thesis RWTH Aachen University Aachen Germany (2009).
[19] S. R. Maity, M. Ceretti, L. Keller, et al. Phys. Rev. Mater., 083604 (2019).
[20] D. Fobes, E. Bauer, J. Thompson, et al. J. Phys.: Condens. Matter 29, 17LT01 (2017)
[21] D. M. Fobes, S. Zhang, S.-Z. Lin, et al. Nature Physics 14, 456–460 (2018).
[22] A. Möchel, Diploma thesis, Friedrich-Wilhelms-Universität Bonn, Germany (2008).
[23] Y. Xiao, Y. Su, M. Meven, et al. Phys. Rev. B 80, 174424 (2009).
[24] W. T. Jin, Wei Li, Y. Su, et al. Phys. Rev. B 91, 064506 (2015).
[25] K. Schreckenbach, J. van Klinken, and J. Last, Proc. 2nd Int. Workshop on Time Reversal Invariance and Parity Violation in Neutron Reactions, Dubna, Russia, May, 1993, (World Scientific Publishing Company, Singapore, 1994), p. 187.
[26] P. Jesinger, A.Kotzle, A.Gagarsky et al, Nucl. Instrum. Meth. A 440, 618 (2000).
[27] F. Gonnenwein, M. Mutterer, A. Gagarski et al, Phys. Lett. B 652, 13 (2007).
[28] G.V. Danilyan, P. Granz, V.A. Krakhotin, et al. Phys. Lett. B 679 25 (2009).
[29] G. V. Danilyan, J. Klenke , V. A. Krakhotin, Yu. N. Kopach, V. V. Novitsky, V. S. Pavlov, and P. B. Shatalov, Phys. At. Nucl. 74, No. 5, 671–674 (2011).
[30] A. Gagarski F. Goennenwein, I.Guseva et al., Phys. Rev. C 93, 054619 (2016).
[31] D. Berikov, V. Hutanu, Yu. Kopatch, et al. JINST 15 P01014 (2020).
[32] Y. Kopatch, V. Novitsky, G. Ahmadov, et al. EPJ Web of Conferences 169, 10 (2018).
[33] Yu.N. Kopatch, V.V. Novitsky, G.S. Ahmadov, et al. ISINN-27 Proc. http://isinn.jinr.ru/proceedings/isinn-27.html (2020).
[34] Yu.N. Kopatch, D.B. Berikov, et al., ISINN-27 Proc. http://isinn.jinr.ru/proceedings/isinn-27.html (2020).
[35] D. Berikov, G. Ahmadov, Yu. Kopatch, et al. Phys. Rev. C 104, 024607 (2021).